On Medical Implant Communication of IR-UWB

Kasun Thotahewa
Monash University
Wellington Road
VIC, 3800, Australia.
kasun.thotahewa@monash.edu

Jean-Michel Redoute
Monash University
Wellington Road
VIC, 3800, Australia.
jean-michel.redoute@monash.edu

Mehmet Rasit Yuce
Monash University
Wellington Road
VIC, 3800, Australia.
mehmet.yuce@monash.edu

ABSTRACT
Impulse Radio-Ultra-Wideband (IR-UWB) is gaining popularity for a variety of short-range Wireless Body Area Network (WBAN) applications. In-body to outside-body communication is one of the possible applications of IR-UWB signals. This paper analyses various aspects related to implant communication of IR-UWB signals, antenna gain characteristics, propagation loss, and Bit Error Rate (BER) variation. The development of an implantable IR-UWB antenna that operates in the frequency range of 3.5-4.5 GHz is discussed. Its operation within the implant environment is described in terms of simulated and measured antenna gain. Experiments that evaluate the path loss and BER characteristics of IR-UWB communication are carried out using pork, which is used as the human tissue simulating material. Experimental results show a path loss variation of more than 90 dB for an in-body propagation distance of 100 mm. The BER experiments show that this IR-UWB system can operate at a BER of 10^{-3} for an in-body propagation distance of 100mm when it is operating at a data rate of 1Mbps.

Categories and Subject Descriptors
C.2.1 Network Architecture and Design - Wireless communication.

General Terms
Measurement, Performance, Design, Experimentation.

Keywords
IR-UWB, Implant communication, BER, Path-loss.

1. INTRODUCTION
Wireless communication of implant devices provides numerous benefits in the area of healthcare monitoring. These include, minimizing restrictions in daily activities, facilitating less invasive surgical procedures, and offering remote control and monitoring [1, 2]. Impulse Radio–Ultra-Wideband (IR-UWB) has drawn attention as a suitable wireless technology for implant Wireless Body Area Network (WBAN) applications due to its unique properties, such as low power transmitter designs, small form factor and high data rate capabilities [2-5]. Figure 1 depicts a typical setup of an in-body to off-body WBAN communication system that transmits data from a wireless capsule located inside the digestive track to an off-body coordinator node. In an IR-UWB based medical communication system, sensor nodes gather vital physiological data from sensors attached to them, and transmit that data over the IR-UWB link using modulation schemes, such as On-Off-Keying (OOK) and Binary Pulse Position Modulation (BPPM). One of the major limiting factors of using IR-UWB technology for in-body communication applications is its high attenuation within the tissue medium [5]. Although lower portion of the UWB transmit spectrum can be utilized for in-body communication to minimize the high tissue absorption, the physical size of antenna will increase.

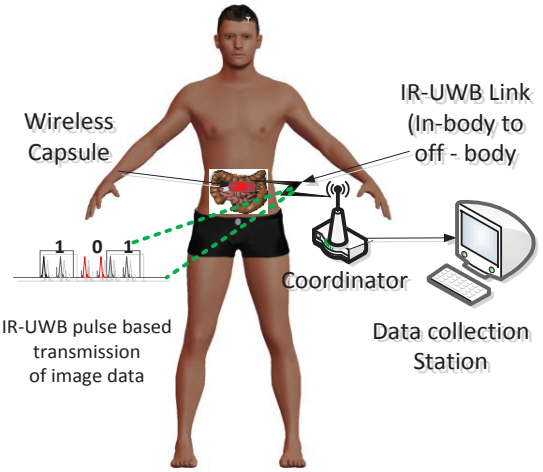

Figure 1. IR-UWB based data transmission from a wireless capsule device to an off-body coordinator node.

The main intention of this paper is to analyze various aspects, such as implant antenna performance, Bit Error Rate (BER) and path loss, related to in-body to off-body communication of IR-UWB signals. An UWB antenna with appropriate matching characteristics plays a vital role in achieving efficient data communication in an implant environment. This paper presents the development of an implantable UWB antenna that can operate inside a wireless capsule. Its performance during operation inside a tissue medium is evaluated in terms of reflection coefficient and

BODYNETS 2014, September 29-October 01, London, Great Britain

DOI 10.4108/icst.bodynets.2014.257120

antenna gain. The performance of the in-body to off-body communication link is evaluated in terms of BER and path loss.

Rest of the paper is organized as follows; Section II describes the design of experimental evaluation of the implantable antenna. Section III describes experimental path loss evaluation for an in-body communication link. Section IV describes the experimental procedure used to evaluate the in-body BER and corresponding results. Finally, Section V concludes the paper.

2. UWB ANTENNA DESIGN

An antenna that demonstrates proper matching characteristics in a highly dissipative medium, such as human tissue, is a key component in a high frequency implantable wireless communication system [7]. Good impedance matching characteristics provide efficient transition of the RF wave from the implantable circuitry into the tissue medium with minimum loss. The antenna presented in this section operates at a 4GHz center frequency with a bandwidth of approximately 1GHz. The 4GHz center frequency is chosen to minimize tissue attenuation and the interference from other wireless technologies, such as 5GHz Wi-Fi, in a practical scenario. The dimensions of the antenna are 13.65×9×1.27 mm, which are compliant with the commercially available capsule sizes used for WCE [1, 8].

The antenna is first developed in a simulation environment using CST Microwave Studio [9]. A human voxel body model comprising of tissue simulating materials is used to simulate the in-body propagation environment. Relative permittivity of the tissue is adjusted according to the incident frequency range of 3.5-4.5 GHz using Cole-Cole approximation equations [12]. Using an insulating material between the dispersive tissue medium and the radiating element of the antenna improves the impedance matching characteristics of an implantable antenna [7, 10]. The radiating element of the antenna used in the simulations, which occupies the lower half of the antenna, is inserted in glycerin for this purpose. Glycerin has a relative permittivity of 50, which is close to the relative permittivity of the surrounding tissue material; hence allows minimal reflections of the electromagnetic wave near the transitional boundaries between the tissue medium and the capsule.

UWB antennas developed based on the electric dipole principal, such as the one shown in [11], are susceptible to changes in the surrounding tissue environment. This is mainly due to the significant effects of dielectric properties of the surrounding tissue on surface currents that appear near the tapered edges of these types of antennas. The wide-slot antenna presented in this paper is designed with a U-shaped feed. It forms a magnetic dipole, which is less susceptible to variations in the near field propagation environment. Figure 2 depicts the simulated antenna model and human body model. The antenna is fabricated on *Rogers TMM 10i* high frequency material. The antenna uses a vertical feed through a 50 Ω Radio Frequency (RF) connector. The bottom copper layer and the outside copper layer surrounding the antenna feed element is connected to the RF signal ground. Figure 3 depicts the fabricated antenna and its important dimensions.

The performance of the antenna is evaluated using the experimental setup shown in Figure 4. The antenna is inserted in a plastic casing with its feed element immersed in a non-flowing glycerin based gel medium as shown in Figure 2. During the experiments, the top side of the plastic casing is sealed with a water resistant material. Pork is used as the tissue simulating material in the experimental setup due to the similarities between pork and human tissue properties at microwave frequencies [13]. Figure 5 depicts the simulated and measured S-parameters of the implanted antenna.

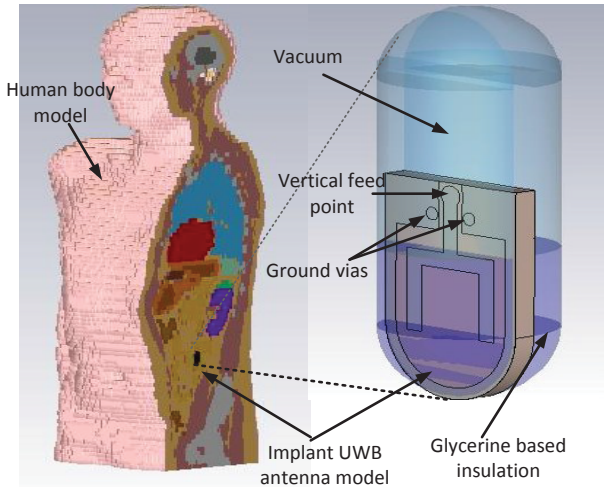

Figure 2. Human body model and UWB antenna model used in the simulations.

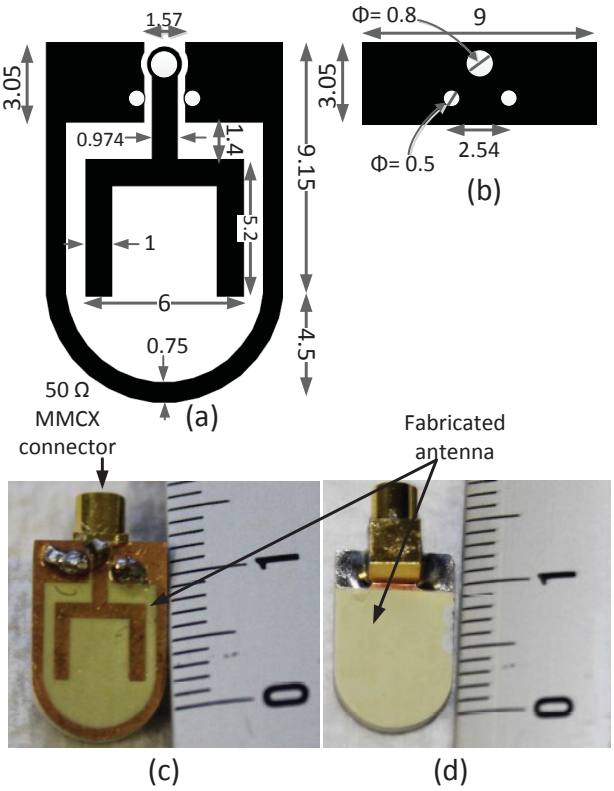

Figure 3. Antenna dimensions in mm (a) front side (b) backside, fabricated antenna (c) front side (b) backside.

The two dimensional polar plots of the simulated and measured far field gain of the antenna at 4GHz are shown in Figure 5. In the simulations, three dimensional far field antenna gain is calculated using (1), and converted into a two-dimensional plot using the gain values at the intersections with the horizontal plane that passes through the center of the antenna feed element.

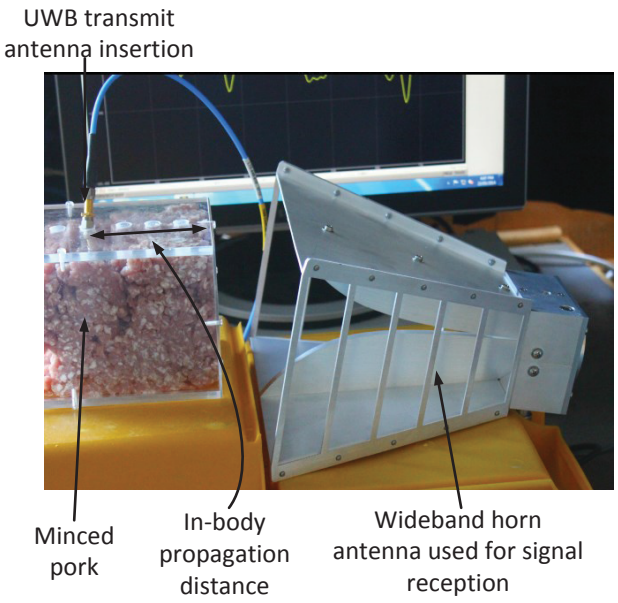

Figure 4. Experimental setup used for S-parameter measurements, antenna gain measurements and path loss measurements.

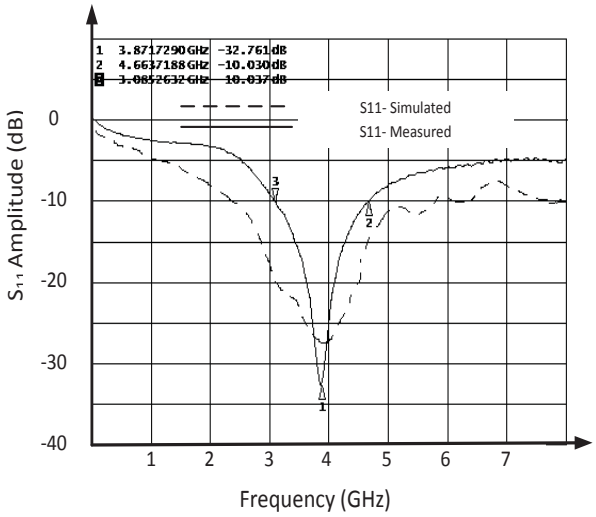

Figure 5. Simulated and measured antenna S_{11} of the implanted UWB antenna.

$$G = 4\pi.\frac{(P_{rad}-P_{tissue})}{P_i} \quad (1)$$

where G is the three dimensional gain, P_{rad} is the power radiated per unit solid angle, P_{tissue} is the power absorbed by tissues within the unit solid angle and P_i is the accepted power of the antenna after the antenna reflections. It should be noted that the antenna gain is obtained after reducing the power absorbed by the surrounding tissue.

The antenna far field is measured in the following manner. Firstly, the UWB implant antenna is inserted in pork as shown in Figure 4. The receiving horn antenna is positioned in the far field of the UWB implant antenna (at a distance of 8 cm from the UWB antenna in this case). The S-parameters (S_{11} and S_{21}) are recorded for this position. This measurement procedure is repeated for twelve positions on a circumference of a circle that is centered on the implanted UWB antenna. Equation (2) is used to calculate the antenna gain after tissue absorption [14].

$$G_m = \frac{|S_{21}|^2}{1-|S_{11}|^2} \quad (2)$$

where G_m is the measured antenna gain, andS_{21}, S_{11} are scattering parameters. Figure 6 depicts the measured and simulated far field gain of the UWB antenna.

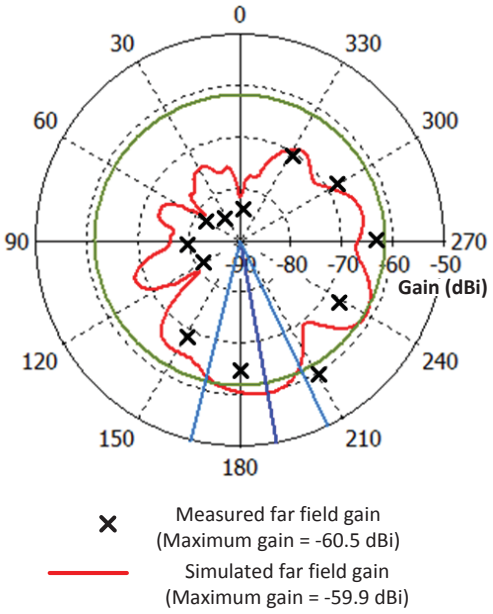

Figure 6. Measured and simulated far field antenna gain.

3. IN-BODY PATH LOSS MEASUREMENT

In-body path loss variation is an important factor that decides the feasibility of IR-UWB for implant communication. Due to the high frequency nature of IR-UWB signals, a significant portion of the transmit power is absorbed by the surrounding tissue. This section analyses the in-body path loss variation of IR-UWB signals in the frequency range of 3.5-4.5 GHz, which belongs to the lower part of the UWB spectrum.

The measurement set up used for path loss evaluation is shown in Figure 4. A wideband horn antenna is used as the receiving antenna for the path loss measurement. Its S-parameters are shown in Figure 7. These two antennas are connected to a Vector Network Analyzer (VNA). Path loss measurements for various transmit-receive separation values are obtained using the following equation [15];

$$PL_{dB} = -|S_{21}|_{dB} \quad (3)$$

where PL_{dB} is the path loss and S_{21} is the forward transmission coefficient.

An input signal power of 0 dBm is used for the excitation of the transmit antenna. Initially, path loss for the free space portion of the propagation channel is obtained by placing the transmit antenna near the meat/ air interface inside the containing tank. Path loss variation for various transmit-receive separations that

are 2 cm apart from each other are measured by changing the transmit antenna insertion location inside meat. Free space path loss component, which is calculated during the initial measurement, is deducted from the path loss values obtained from later measurements in order to calculate the measured in-body path loss component. Figure 8 depicts the path loss variation at 4 GHz with in-body propagation distance.

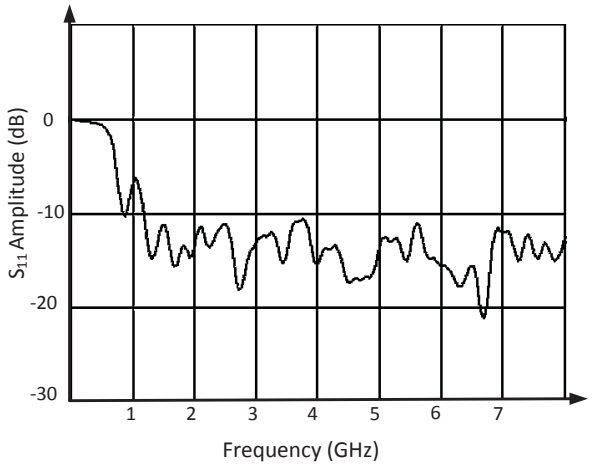

Figure 7. S_{11} of the horn antenna used for UWB reception.

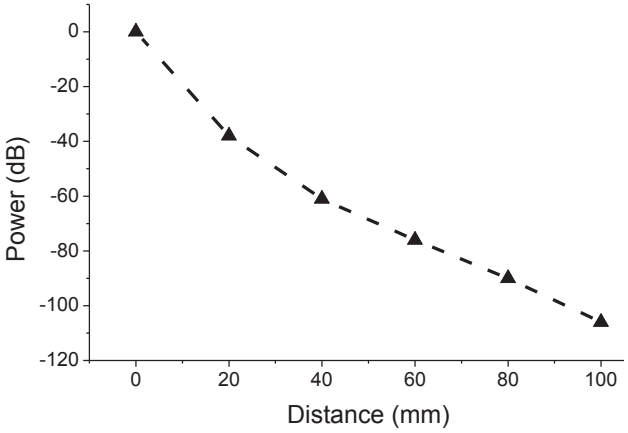

Figure 8. Measured in-body path loss variation with propagation distance at 4 GHz.

It can be seen that the in-body signal power rapidly decays with the in-body propagation distance. This is mainly due to high tissue absorbtion at UWB frequencies. The measured path loss variation agrees well with our previously published path loss model presented in [16]. Figure 9 depicts the measured path loss variation over the frequency range of 3.5 GHz to 4.5 GHz, which is the target frequency range of the antenna. This measurement is taken for an in-body propagation distance of 60 mm.

4. BIT ERROR RATE VARIATION FOR THE IN-BODY COMMUNICATION OF IR-UWB

Figure 10 depicts the experimental set up used for evaluation of BER. UWB transmitter and receiver nodes shown in [17, 18] is used for these experiments. During the experiments, a single UWB transmitter node is used to transmit a known bit pattern with a length of 10^8 bits using the implant UWB antenna that is inserted in pork. The transmitter node is set to transmit IR-UWB pulses at 100 MHz PRF and a peak transmit power of -25.12 dBm, which is higher than the Federal Communications Commission (FCC) compliance spectral mask of -41.3 dBm/MHz for indoor propagation of UWB signals. Use of higher transmit power can be justified by the fact that the corresponding indoor transmit power after the tissue absorption falls within the FCC allowed spectral mask [7, 16].

Data is modulated with IR-UWB pulses using OOK modulation. BER is evaluated for three different data rates as shown in Table 1. Data rates are changed by changing the number of IR-UWB pulses sent to represent a data bit. When coordinator node receives data from the sensor node, it transfers the received data to a Matlab program that calculates BER. BER is measured for varying distances between the transmit and receive antennas. Five BER measurements are taken for each transmit-receive separation and average is taken as the final BER. This data transmission forms a transmit-only medium access mechanism as discussed in [19]. During the initiation of the data transmission period, the coordinator node is initiated before the transmitter node in order to detect the start of data transmission. Figure 11 depicts the BER variation with in-body propagation distance. BER that occurs due to propagation of the signals through the small free space propagation distance is considered constant for all the BER measurements. Hence, the BER is plotted only against the in-body propagation distance in Figure 11.

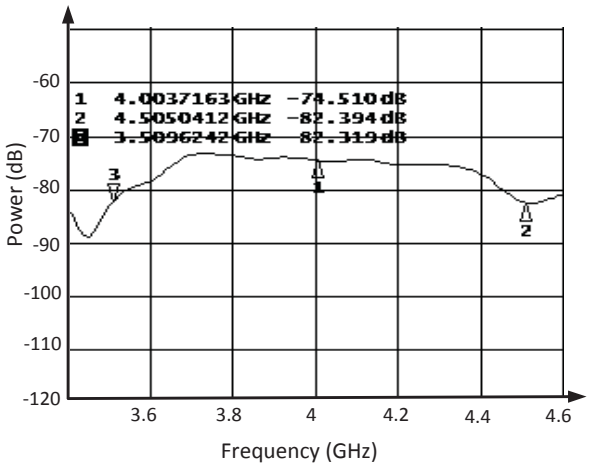

Figure 9. In-body path loss variation over the target frequency range of the UWB implant antenna for an in-body propagation distance of 60 mm.

Table 1. Relationship between the data rates and the number of IR-UWB pulses that represents a data bit.

Data rate	Number of IR-UWB pulses that represent a data bit (PRF=100 MHz)
5 Mbps	20
2 Mbps	50
1 Mbps	100

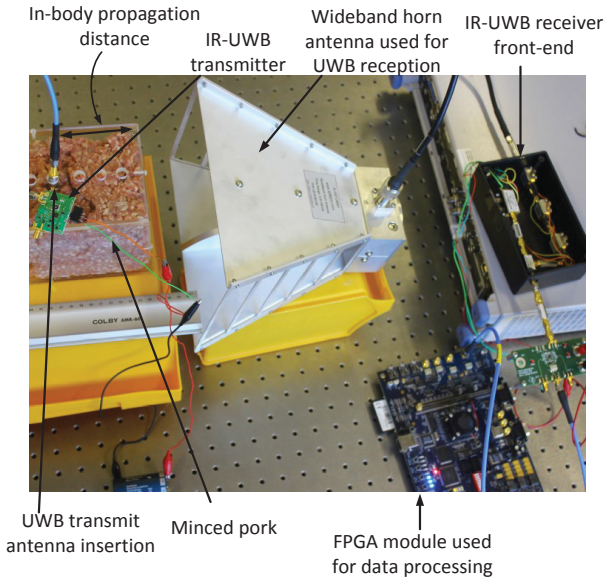

Figure 10. Experimental set up used for evaluation of BER.

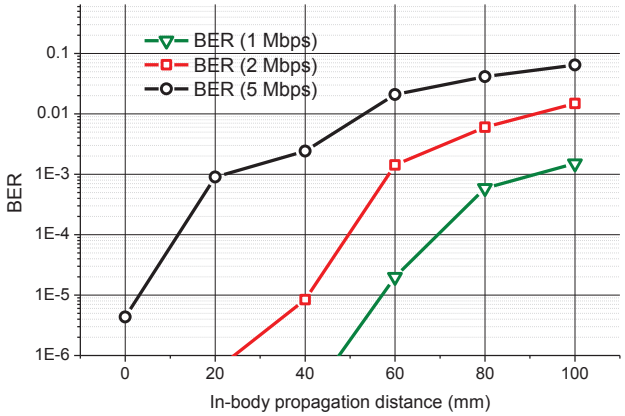

Figure 11. Experimental BER variation with in-body propagation distance.

It can be seen from Figure 11 that the recorded BER values follow a logarithmic decay as the transmit – receive separation increases. The BER variation demonstrates an inverse relationship to the data rate. This can be explained as follows; lower data rates correspond to sending higher number of IR-UWB pulses to represent a data bit. Considering the fact that the random effects, such as selective fading and diffraction, of the propagation channel on individual IR-UWB pulses are mutually independent, transmitting higher number of pulses increases the probability of detection [20]. This condition is valid given that the receiver antenna receives adequate amount of signal power. Hence, data transmission at low data rates demonstrates low BER values. The inconsistent variation of BER for an in-body separation distance of 40 mm is due to the irregular distribution of pork in the sample used for the experiment and variation of relative permittivity in different types of tissues. The recorded BER value for 0 mm in-body propagation distance at 5 Mbps data rate is due to the BER that occur because of the small free-space separation between the transmit and receive antennas. This BER variation agrees with the work presented in [3] for a similar experiment. BER measurements in this paper are slightly lower due to the better performance of the implant antenna compared to that in [3].

5. CONCLUSION

This paper presents in-body evaluation of an IR-UWB based medical communication system. The design and fabrication of an implantable miniature UWB antenna is presented. Its in-body performance is experimentally evaluated in terms of return loss and antenna gain. This antenna shows a gain of -60 dBi when it is fully implanted in meat. This paper also presents in-body path loss variation for IR-UWB signals. Path loss is experimentally evaluated using pork as tissue simulating material. These experiments show a path loss of more than 90 dB for an in-body propagation distance of 100m. In-body BER experiments carried out in this paper shows that this IR-UWB communication system can operate at a satisfactory data rate of 10^{-3} for an in-body propagation distance of 100mm.

6. ACKNOWLEDGMENTS

The authors would like to thank Dr. Tharaka Dissanayake for his help in designing the UWB antenna used for the high frequency simulations. Also, special thank should be given to Monash e-Research Centre, Monash University, Australia for their cooperation in assisting this work by providing the high performance computing facility for the computationally intensive simulations.

This work is supported in part by Monash Seed and Monash Researcher Accelerator grants. Mehmet R. Yuce's work was supported by Australian Research Council Future Fellowships Grant FT130100430.

7. REFERENCES

[1] M. R. Yuce and T. Dissanayake "Easy to swallow antenna and propagation," IEEE *Microwave Magazine*, vol. 14, pp. 74-82, June 2013.

[2] M. Chae, Z. Yang, M.R. Yuce, L. Hoang, and W. Liu, "A 128-Channel 6 mW Wireless Neural Recording IC with Spike Feature Extraction and UWB Transmitter," *IEEE Transactions on Neural Systems and Rehabilitation Engineering*, vol.17, no.4, pp.312-321, Aug. 2009.

[3] D. Anzai, K. Katsu, R. Chavez-Santiago, W. Qiong, D. Plettemeier, W. Jianqing, and I. Balasingham, "Experimental Evaluation of Implant UWB-IR Transmission With Living Animal for Body Area Networks," *IEEE Transactions on Microwave Theory and Techniques*, vol. 62, pp. 183-192, 2014.

[4] E. Pancera, "Medical applications of the Ultra Wideband technology," *Antennas and Propagation Conference (LAPC)*, pp. 52-56, 2010.

[5] J. Shi, D. Anzai, and J. Wang, "Link budget analysis of in-body to on-body UWB low band communications for capsule endoscope," Proceedings of the 7th International Conference on Body Area Networks, Oslo, Norway, 2012.

[6] K. M. Thotahewa, J-M, Redoute and M. R. Yuce, Ultra Wideband Wireless Body Area Networks, Springer, ISBN 978-3319052861, May 2014.

[7] T. Dissanayake, K.P. Esselle, and M.R. Yuce, "Dielectric loaded impedance matching for wideband implanted antennas," *IEEE Transactions on Microwave Theory and Techniques*, vol.57, no.10, pp.2480-2487, Oct. 2009.

[8] J. L. Toennies, G. Tortora, M. Simi, P. Valdastri, and R. J. Webster, "Swallowable medical devices for diagnosis and surgery: the state of the art", *IMechE Proceedings* , vol.224, no.7, pp.1397-1414, 2010.

[9] www.cst.com, 2014.

[10] K.M.S. Thotahewa, J.-M. Redoute, and M.R. Yuce, "SAR, SA, and Temperature Variation in the Human Head Caused by IR-UWB Implants Operating at 4 GHz," *IEEE Transactions on Microwave Theory and Techniques*, vol.61, no.5, pp.2161-2169, May 2013.

[11] H. Bahrami, B. Gosselin, and L. A. Rusch, "Design of a miniaturized UWB antenna optimized for implantable neural recording systems," *IEEE 10th International New Circuits and Systems Conference*, pp. 309-312 , 2012.

[12] S. Gabriel, R. W. Lau, and C. Gabriel, "The dielectric Properties of Biological Tissues: III. Parametric Models for the Dielectric Spectrum of Tissues," *Physics in Medicine and Biology*, vol. 41, no. 11, pp. 2271–2293, 1996.

[13] M. Vallejo, J. Recas, P. del Valle, and J. Ayala, "Accurate Human Tissue Characterization for Energy-Efficient Wireless On-Body Communications," Sensors, vol. 13, pp. 7546-7569, 2013.

[14] T. Prakoso, R. Ngah, and T. A. Rahman, "Representation of antenna in two-port network s-parameter," *IEEE International RF and Microwave Conference*, pp. 293-297, 2008.

[15] K. Lopez-Linares Roman, G. Vermeeren, A. Thielens, W. Joseph, and L. Martens, "Characterization of path loss and absorption for a wireless radio frequency link between an in-body endoscopy capsule and a receiver outside the body," *EURASIP Journal on Wireless Communications and Networking*, vol. 2014, pp. 1-10, Feb 2014.

[16] K. M. S. Thotahewa, J. M. Redoute, and M. R. Yuce, "Electromagnetic power absorption of the human abdomen from IR-UWB based wireless capsule endoscopy devices," *IEEE International Conference on Ultra-Wideband (ICUWB)*, pp. 79-84, 2013.

[17] K. M. S. Thotahewa, J. M. Redoute, and M. R. Yuce, "Implementation of a dual band body sensor node," *IEEE MTT-S International Microwave Workshop Series on RF and Wireless Technologies for Biomedical and Healthcare Applications*, pp. 1-3, 2013.

[18] M. R. Yuce, K. M. Thotahewa, J-M. Redoute, Ho Chee Keong, "Development of low-power UWB body sensors," *IEEE International Symposium on Communications and Information Technologies* (ISCIT), pp. 143-148, October 2012.

[19] K. Ho Chee, K. M. S. Thotahewa, and M. R. Yuce, "Transmit-Only Ultra Wide Band Body Sensors and Collision Analysis," *IEEE Sensors Journal,* vol. 13, pp. 1949-1958, 2013.

[20] K. Thotahewa, J. Khan, and M. Yuce, "Power Efficient Ultra Wide Band Based Wireless Body Area Networks with Narrowband Feedback Path," *IEEE Transactions on Mobile Computing,* vol. PP, pp. 1-1, 2013.